

PACS 63.20.Dj, 73.40.Lq

## **Investigation of electron-phonon interaction in bulk and nanostructured semiconductors**

**A.M. Yaremko<sup>1</sup>, V.O. Yukhymchuk<sup>1</sup>, V.M. Dzhagan<sup>1</sup>, M.Ya. Valakh<sup>1</sup>, Yu.M. Azhniuk<sup>2</sup>, J. Baran<sup>3</sup>, H. Ratajczak<sup>3</sup>, M. Drozd<sup>3</sup>**

<sup>1</sup> *V. Lashkaryov Institute of Semiconductor Physics, NAS of Ukraine, 45, prospect Nauky, 03028 Kyiv, Ukraine*

<sup>2</sup> *Institute of Electron Physics, NAS of Ukraine, 21, Universitetska str., 88000 Uzhgorod, Ukraine*

<sup>3</sup> *Institute of Low Temperatures and Structural Research, Polish NAS, Okolna, 2, 50-422 Wroclaw, Poland*

*E-mail: yaremko@isp.kiev.ua*

**Abstract.** In this paper, the problem of electron-phonon interaction (EPI) in semiconductor crystals and quantum dots (QDs) is considered. It is shown that the model of strong EPI developed for organic molecular crystals can be successfully applied to bulk and nanosized semiconductors. The idea of the approach proposed here is to describe the experimental Raman (or absorption) spectra containing the phonon replicas theoretically by varying the EPI constant. The main parameter of the theoretical expression describing the experimental spectrum is the ratio of EPI constant to the frequency of the corresponding phonon mode. Based on the experimental and theoretical results, we have found that decreasing the size of CdS<sub>x</sub>Se<sub>1-x</sub> QDs embedded in borosilicate glass matrix results in some enhancement of electron-phonon interaction.

**Keywords:** electron-phonon interaction, Raman scattering, quantum dots.

Manuscript received 28.02.07; accepted for publication 24.04.07; published online 19.10.07.

### **1. Introduction**

In the past two decades, an intense experimental and theoretical researches on structural and optical properties of semiconductor nanostructures were caused by the interest to fundamental physical processes in these structures and their application in devices of novel types. The spatial confinement of electrons and phonons in nanostructures has a crucial effect on their properties [1]. One of the important characteristics of both bulk and nanosized semiconductors is electron-phonon interaction (EPI). The magnitude of EPI in semiconductor structures strongly affects the electron transport, inelastic light scattering, response of the electronic system to electromagnetic waves and other characteristics. The influence of spatial confinement on the EPI value was studied theoretically [1-3] and experimentally [1, 4, 5]. However, there exist discrepancies in the results obtained concerning the value of EPI, and no clear conception has been formulated yet in this issue.

In the view of all stated above, the problem of variation of the EPI value on evolution of semiconductor from bulk ones to nanostructures of various sizes is approached once more in this work.

The response features of a physical system to the action of electromagnetic waves are known to depend on the value of EPI. EPI can be characterized as weak or strong depending on the ratio of the EPI constant  $\chi_s$  to the corresponding phonon frequency  $\Omega_s$ :  $\beta_s = \chi_s/\Omega_s$ .

Theoretical consideration of EPI in bulk semiconductor crystals is often limited to the perturbation theory and describes first and second phonon replicas in the Raman or absorption spectra [6]. In the case of organic crystals including those with hydrogen bonds, this approach is not sufficient because they are frequently characterized by  $\beta_s \geq 1$ , which causes multiphonon replicas. This circumstance was emphasized as early as in the works by Davydov and coworkers [7]. The similar problem arises when the interactions of high- and low-frequency vibrations in molecular crystals are studied. Such a problem for the intramolecular high-frequency ( $\sim 2500 \dots 3000 \text{ cm}^{-1}$ ) vibrations in the hydrogen bonded crystal was considered in Refs [8, 9].

It should be also noted that in some semiconductor compounds, especially of A<sup>2</sup>B<sup>6</sup> type, such as CdS, ZnO *etc.*, the multiphonon replicas were also observed revealing strong EPI in them. Therefore in this work,

when analyzing the experimental Raman spectra, we have equally approached the problem of EPI both for organic and inorganic compounds and made some general conclusions concerning the quantum confinement effect on the EPI value. The idea of our approach is to describe theoretically the experimental Raman (IR) spectrum with multiphonon replicas by varying the  $\beta_s$  value and to conclude concerning EPI from the value of  $\beta_s$ , when the best fitting of both spectra is achieved. Theoretical description of Raman spectra is convenient to be made by using the theory of strong EPI that allows to consider the contribution of several phonons to the spectrum by using a single expression.

## 2. Raman (IR) band shape, short theory

### 2.1. Frenkel type excitons in bulk crystals

It should be noted that in the crystal with phonon interaction, electrons were distributed over various energetic bands. Under excitation of the crystal by irradiation with the frequency (energy) that is close to the energy of interband transition ( $E_g$ ), part of electrons is excited to more higher energy states. This process is observed in absorption spectra, for example, as sharp peaks (exciton maxima) near the absorption edge.

In semiconductor crystals, the excited electron in the conduction band and the hole created in the valence band, according to Wannier's model, are located on the distance  $R_{ex}$  one from another, and interaction of phonons with each of them must be considered separately.

For molecular type crystals, the excited electron and created hole are located on the same atom or molecule. Therefore, the phonon interacts with this pair (Frenkel exciton), and one can say about the exciton-phonon interaction.

In this work, we study also quantum dots (QDs), the sizes of which are 3 to 5 nm, and they are similar to big molecules. Therefore, the theoretical approach developed for molecular type crystals can be enough adequate for the QD structures, too. Moreover, our calculations show that the Raman spectra of pure semiconductor crystals are described in this approach well enough, too.

We present below only a final expression describing energy and intensity for the case of strong electron-phonon interaction (some formal theoretical approaches you can see in [8-10]). The results were obtained in the approximation when the electron band is sufficiently narrow (*i.e.*, the exchange term value is smaller than that of the Coulomb interaction  $|M^v| \ll |D^v|$ ). The Hamiltonian describing the system of electron excitations in the crystal interacting with phonons is given by [8]

$$H = \sum_{n,\nu} E_{n\nu}(R) a_{n\nu}^+ a_{n\nu} + \sum_{s,q} \Omega_{sq} b_{sq}^+ b_{sq}, \quad (1)$$

where  $E_{n\nu}(R), a_{n\nu}^+, a_{n\nu}$  are the energy and Bose operators of creation and annihilation of electron excitation in the crystal, respectively;  $\nu$  enumerates the quasi-degenerated states of a molecule; the second sum in Eq. (1) describes the phonon system with  $s, q$  being the phonon branch number and wave vector, respectively;  $R$  characterizes the deviation of the molecule coordinate, shift and libration, from the equilibrium position.

Taking into account the small deviation from the equilibrium position, the Hamiltonian (1) can be written as follows [8]:

$$H = \sum_{n,\nu} E_{n\nu}(0) a_{n\nu}^+ a_{n\nu} + \frac{1}{\sqrt{N}} \sum_{n\nu, sq} \chi_{sq}^{n\nu} a_{n\nu}^+ a_{n\nu} \varphi_{sq} + \sum_{s,q} \Omega_{sq} b_{sq}^+ b_{sq}, \quad \varphi_{sq} = b_{sq} + b_{s,-q}^+ \quad (2)$$

that after the unitary transformation [8] is reduced to a simple form

$$H = \sum_{n,\nu} \varepsilon_{n\nu} A_{n\nu}^+ A_{n\nu} + \sum_{sq} \Omega_{sq} \beta_{sq}^+ \beta_{sq}, \quad (3)$$

where

$$\varepsilon_{n\nu} = E_{n\nu}(0) - N^{-1} \sum_{sq} \Omega_{sq}^{-1} |\chi_{sq}^{n\nu}|^2 \quad (4)$$

is a new energy of electron excitations renormalized due to the interaction of electron with the lattice vibrations.

The intensity of light absorption (or the Raman scattering) can be expressed in the Fourier component of the retarded Green function expressed by the  $a_{n\nu}, a_{n\nu}^+$  operators. The corresponding spectral profiles are described as follows [8, 9]:

$$I(\omega) \approx \text{Im} \left[ - \sum_{\nu, \mu} d_{n\nu} d_{n\mu}^* G_n^{v\mu}(\omega) \right], \quad G_n^{v\mu}(\omega) = \delta_{v\mu} G_n^v(\omega), \quad (5)$$

$$G^v(\omega) = -i \int_0^\infty dt \exp[i(\omega - \varepsilon_{n\nu} + i\gamma_\nu)t + g_{n\nu}(t)]. \quad (6)$$

In Eq. (6), the positive value of  $\gamma_\nu$  characterizes the natural damping of  $\varepsilon_{n\nu}$  given by Eq. (4). The function  $g_{n\nu}(t)$  with a complex dependence on the lattice frequencies  $\Omega_{sq}$  and coupling constants  $\chi_{sq}^{n\nu}$  is determined as

$$g_{n\nu}(t) = N^{-1} \sum_{sq} |\chi_{sq}^{n\nu}|^2 \Omega_{sq}^{-2} \times \{ [n_{sq} + 1] \exp(-i\Omega_{sq} t) + n_{sq} \exp(i\Omega_{sq} t) - [2n_{sq} + 1] \}, \quad (7)$$

where  $n_{sq}$  is the occupation number of the vibrational state with the frequency  $\Omega_{sq}$ .

In the further analysis, we use Eqs (5-7) but neglect the dependence on the wave vector  $q$  by putting  $\Omega_{sq} = \Omega_s$  for the lattice phonon frequencies and  $\chi_{sq}^{n\nu} = \chi_s^\nu$  for the coupling constants.

Eqs (5)-(7) describe the new *real* electron-phonon states, the oscillator strength of which depends on both the exciton dipole moment, Eq. (5), and the coupling constant factors, Eq. (7). Therefore, the intensity of corresponding components of the multiplet, Eqs (5-7), ruled this ‘‘coupling’’ factor too, and the greater this factor the more components will be observed. The Raman scattering intensity or the absorption coefficient, *i.e.* the band shape of the spectrum, depends on such parameters as the coupling constants  $\chi_s^\nu$ , lattice frequencies  $\Omega_s$  and damping constant  $\gamma_\nu$ . The role of these parameters can be understood in the numerical analysis of different cases.

As an example, we present the low-temperature spectrum, when only one type of lattice phonon interacts with the electron system (Fig. 1).

## 2.2. The Wannier type excitons in bulk semiconductors

In semiconductor crystals, the electron bands are broad and comparable with the bandgap. The electron band energy  $\varepsilon(k)$  in  $k$ -space can be presented as an expansion in a series on the space harmonics (several of them are sufficient):

$$\varepsilon_k^\nu = \varepsilon_0^\nu + \sum_{n=1}^p [M_{n,x}^\nu \cos(nk_x a_x) + M_{n,y}^\nu \cos(nk_y a_y) + M_{n,z}^\nu \cos(nk_z a_z)]. \quad (8)$$

Here,  $k_i$ ,  $a_i$  ( $i = x, y, z$ ) are the components of the wave vector and lattice vector, respectively;  $M_{n,i}^\nu$ ,  $\varepsilon_0^\nu$  are the parameters of the  $\nu$ -th electron band,  $\nu = 0, 1$ ;  $n$  is the number of harmonics.

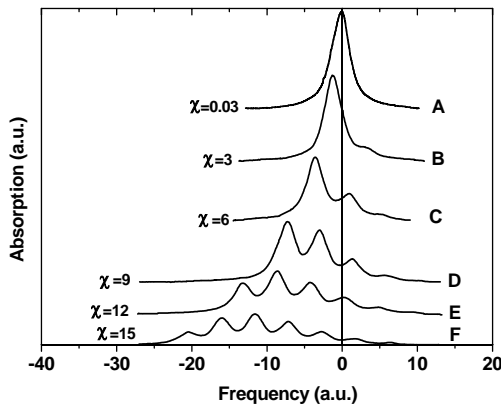


**Fig. 1.** Effect of electron-phonon interaction on the band shape for the Frenkel exciton.

The many-particle description of the Wannier excitons is a rather complicated problem [10, 11] and, for the case of two bands, the absorption of light corresponding to the transition between valence and conduction bands, is described as follows:

$$I(\omega, Q) \sim -2|p^{0,1}|^2 \text{Im} \frac{f^{0,1}(\omega, Q)}{1 - a_Q^* f^{0,1}(\omega, Q)}, \quad (9)$$

where the constant  $a_Q = a = 2V_Q^{0,1,0,1} - V_0^{1,0,0,1}$  is the difference between the exchange and Coulomb interaction of two electrons ( $Q \rightarrow 0$ ).

The complex function  $f^{0,1}(\omega, Q)$  is written as follows:

$$f^{0,1}(\omega, Q) = \frac{1}{N} \sum_k \frac{(n_k^0 - n_{k-Q}^1)}{\omega + \varepsilon_k^0 - \varepsilon_{k-Q}^1 + i\gamma} = f_1(\omega, Q) + if_2(\omega, Q), \quad (10)$$

where  $n_k^\nu$  is an occupation number of an electron in the corresponding band and  $\gamma$  is a damping constant.

The spectral distribution of Eq. (9) depends on the structure of the crystal bands  $\varepsilon_k^\nu$ , and the ratio of the band width to the Coulomb interaction constant  $a$ . The typical case is shown in Fig. 2, where the energy bands in the  $k$ -space are described by Eq. (8) using only one harmonic,  $n = 1$ . We observe a strong narrow peak at  $a = -0.5$  and practically no absorption for another band states. In the case  $a > -0.3$  in parallel with the exciton peak, the observable intensity in all the bands occurs.

These results demonstrate that, for the case when the Coulomb interaction parameter  $a$  is greater than the band width ( $M_i < a$ ), the predominant part of the absorption intensity is concentrated in the strong narrow exciton peak, and the situation becomes close to the Frenkel exciton case. Therefore, for the crystals where the excitons are observed as intense narrow peaks it is

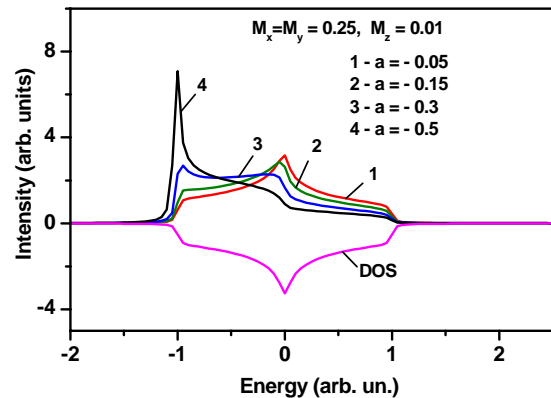


**Fig. 2.** Dependence of the crystal absorption on the  $a$  parameter for a quasi-two-dimensional band.

reasonable to apply Eqs (5–7) for the analysis of the exciton-phonon interaction, at least at a qualitative level.

### 3. Experimental results and discussion

The samples investigated were  $\text{CdS}_x\text{Se}_{1-x}$ , CdSe and CdS QDs embedded in a borosilicate glass matrix as well as bulk CdS and  $\text{CdS}_x\text{Se}_{1-x}$  crystals with the composition  $x$  close to that in the QDs.

The Raman spectra were measured with a DFS-24 double grating spectrometer (LOMO) at room temperature. Discrete lines of an  $\text{Ar}^+$ -laser were used to excite the spectra. The signal was registered with a  $\Phi\text{ЭY-136}$  photomultiplier operating in the photon counting mode. The known frequencies of the discharge lines of the  $\text{Ar}^+$ -laser served for precise measurements of the Raman band frequencies.

In Fig. 3, as an example, the Raman spectrum [12] of perfect CdS crystal is shown. It is clearly seen that several first peaks are well enough fitted by using only one coupling constant  $\chi'_s$  parameter (lattice frequencies  $\Omega_s = 304 \text{ cm}^{-1}$ ,  $\beta_s = \chi'_s / \Omega_s = 2.6$ ). But for 5-8 peaks, the effect of electron band on intensity of peaks is important. This situation will be discussed in detail elsewhere.

Fig. 4 (curve 1) shows the experimental Raman spectrum from the  $\text{CdS}_x\text{Se}_{1-x}$  QDs in the borosilicate matrix and the corresponding theoretical modeling. Only part of the spectrum was shown to demonstrate more clearly the influence of  $\chi_s$  and  $\Omega_s$  values on the theoretical curve. The best fitting was achieved for curve 2. When increasing the EPI constant  $\chi_s$  and fixed phonon frequency  $\Omega_s$  (curve 3), the relative intensity of the second-order band arises. The increase of the latter also occurs for the fixed  $\chi_s$  and the reduction of  $\Omega_s$  (curve 4). The phonon frequency decrease can be caused by both the phonon confinement and variation of chemical composition of the QDs. These two effects can be reliably distinguished only if both CdSe- and CdS-related bands are observed in the experimental spectrum. Then, along with the changes in the band frequency, the changes of the band intensities are used to derive the true origin of the frequency changes observed.

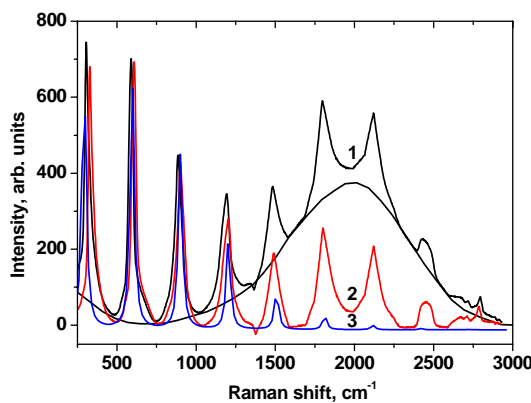


**Fig. 3.** Raman spectrum for CdS crystal (see [13]) (1), the same but without luminescence (2), theoretical spectrum (3).

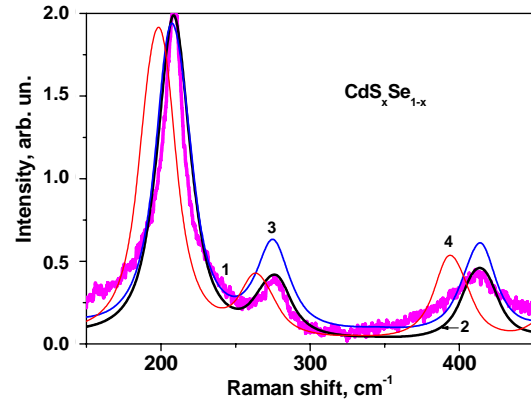


**Fig. 4.** Experimental Raman spectrum of  $\text{CdS}_{1-x}\text{Se}_x$  QDs and its theoretical fitting by varying  $\chi_s$  and  $\Omega_s$ .

Fig. 5 (curve 1) shows the experimental Raman spectrum from  $\text{CdS}_{0.38}\text{Se}_{0.62}$  QDs in the borosilicate matrix and the corresponding theoretical modeling. The first-order Raman spectrum of  $\text{CdS}_{1-x}\text{Se}_x$  solid solutions is known to comprise two main modes: CdSe-like  $\text{LO}_1$  and CdS-like  $\text{LO}_2$ . Beside them, the second-order modes of CdSe-like and CdS-like LO vibrations can appear in the spectrum as well as modes with frequencies equal to the sum or difference of two main modes. For bulk crystals, the frequency and intensity of all these bands depend only on the alloy composition  $x$ . The phonon frequencies in the QDs of the same composition  $x$  can differ from the bulk values due to the effects of quantum confinement and matrix-induced hydrostatic stress.

The results of theoretical fitting of the experimental Raman spectra, shown in Fig. 5, were obtained by variation of the EPI constant value  $\chi_s$ . As clear from Fig. 5, a rather good fitting is achieved simultaneously for both the first- and second-order bands as well as for those corresponding to sums and differences of the first-order phonon frequencies. The shape of the theoretical curve is crucially determined by the value of  $\beta_s = \chi'_s / \Omega_s$  equal to 1.01 and 1.03 for the CdSe- and CdS-like modes, respectively.

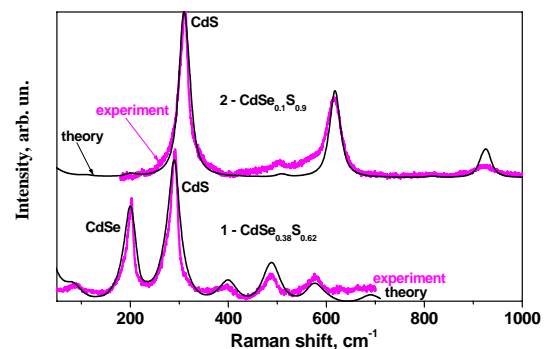


**Fig. 5.** Experimental and theoretical Raman spectra of  $\text{CdS}_{1-x}\text{Se}_x$  QDs with different chemical compositions  $x$ .

In Fig. 5 (curve 2), the experimental and theoretical spectra for the sample with QDs of different composition ( $\text{CdS}_{0.9}\text{Se}_{0.1}$ ) and smaller size are shown. In this case, the first- and higher-order CdSe-like bands are not observed in the experimental spectrum. Simultaneously, we observe the replicas of the CdS-like mode up to the third order. The latter fact can be an evidence for the stronger EPI in the QDs of a smaller size. Indeed, it was shown in Ref. [2] that the EPI enhancement caused the increase of the first-to-second order band intensity ratio for both modes. The best fitting of the spectrum in Fig. 5 (curve 2) was achieved at  $\chi_s / \Omega_s = 1.82$  for the CdS-like mode.

The proposed method of assessing the EPI magnitude can be applied not only to semiconductor structures where EPI occurs predominantly through the Fröhlich potential. The results of the same fitting procedure, which we have obtained for nc-Si, also indicate the EPI enhancement with the decrease of nanocrystallite size and agree with the results of Ref. [13].

#### 4. Conclusions

An estimation method of the EPI magnitude in semiconductor nanostructures was proposed. The method is based on the application of the model of strong EPI to describe the experimental Raman (IR) spectra. It allows them to be described by a single analytic expression in the case when the spectrum is formed by several phonons. The idea of the approach is to describe theoretically the experimental Raman (IR) spectrum containing multiphonon replicas by varying the  $\beta_s$  value and to conclude about the EPI multitude from the value of  $\beta_s$ , at which the best fitting of both spectra is achieved. The developed method is shown to be applicable not only to polar semiconductors but also for covalent ones, in particular, for nc-Si and nc-Ge.

#### References

1. V.V. Mitin, V.A. Kochelap, M.A. Strosio, *Quantum Heterostructures. Microelectronics and Optoelectronics*. Cambridge University Press, Cambridge, 1999.
2. M.C. Klein, F. Hache, D. Ricard, C. Flytzanis, Size dependence of electron-phonon coupling in semiconductor nanospheres: the case of CdSe // *Phys. Rev. B* **42**, p. 11123-11132 (1990).
3. M. Chamarro, C. Gourdon, P. Lavallard, O. Lublinskaya, A.I. Ekimov, Enhancement of electron-hole exchange interaction in CdSe nanocrystals: a quantum confinement effect // *Phys. Rev. B* **53**, p. 1336-1342 (1996).
4. V. Spagnolo, G. Ventruti, G. Scamarcio, M. Lugarà, G.C. Righini, Fröhlich electron-phonon interaction in  $\text{CdS}_x\text{Se}_{1-x}$  nanocrystals // *Superlattices and Microstructures* **18**, N2, p. 113-119 (1995).
5. M. Cardona, G. Guntherodt, *Light Scattering in Solids*, VI. Springer Verlag, Berlin, 1991, p. 431.
6. R. Zeyher, Theory of multiphonon Raman spectra above the energy gap in semiconductors // *Solid State Commun* **16**, p. 49-52 (1975).
7. A.S. Davydov, *Theory of Molecular Excitons*. Nauka, Moscow, 1968.
8. H. Ratajczak, A.M. Yaremko, Theory of profiles of hydrogen stretching infrared bands of hydrogen-bonded solids. Model of strong coupling between the high-frequency hydrogen stretching vibration and low-frequency phonons // *Chem. Phys. Lett.* **243**, p. 348-355 (1995).
9. A.M. Yaremko, H. Ratajczak, J. Baran, A.J. Barnes, E.V. Mozdor, B. Silvi, Theory of profiles of hydrogen bond stretching vibrations: Fermi-Davydov resonances in hydrogen-bonded crystals // *Chem. Phys.* **306**, p. 57-70 (2004).
10. W. Hanke, L.J. Sham, Many-particle effects in the optical spectrum of a semiconductor // *Phys. Rev. B* **21** p. 4656-467 (1980).
11. G. Onida, L. Reining, A. Rubio, Electronic excitations: density-functional versus many-body Green's-function approaches // *Rev. Mod. Phys.* **74**, p. 601-659 (2002).
12. R.C.C. Leite, J.F. Scott, T.C. Damen, Multiphonon resonant Raman scattering in CdS // *Phys. Rev. Lett.* **22**, p. 780-782 (1969).
13. P. Mishra, K.P. Jain, First- and second-order Raman scattering in nanocrystalline silicon // *Phys. Rev. B* **64**, 073304-04 (2001).